Integration of sar and optical dense time series for land cover monitoring

Molijn, R. A.; Iannini, L.; Hanssen, R. F.; Van Leijen, F. J.; Lamparelli, R.; Coutinho, A.

DOI
10.1109/IGARSS.2017.8127960

Publication date
2017

Document Version
Final published version

Published in
2017 IEEE International Geoscience and Remote Sensing Symposium

INTEGRATION OF SAR AND OPTICAL DENSE TIME SERIES FOR LAND COVER MONITORING

R.A. Molijn [1], L. Iannini [1], R.F. Hanssen [1], F.J. van Leijen [1], R. Lamparelli [2], A. Coutinho [3]

[1] Delft University of Technology, The Netherlands, [2] UNICAMP, Brazil, [3] EMBRAPA, Brazil

ABSTRACT

Multi-temporal and multi-sensor solutions are essential to increase timeliness and reliability of land monitoring systems. This paper advocates the exploitation of the temporal contextual information provided by temporally dense SAR and optical data series series through the use of a Hidden Markov model (HMM)-based approach. An efficient strategy to incorporate the C-Band SAR data into the HMM framework, relying so far on Landsat, will be debated and assessed over a dynamic agricultural scenario, i.e. characterized by high temporal and spatial diversity in cropping practices. The site is located in the state of São Paulo (Brazil), where recent ground surveying activities has been conducted.

Index Terms— Land cover mapping, Landsat, C-band SAR, time series processing, sensor assimilation.

1. INTRODUCTION

Land conversion processes have direct and indirect impacts on small and large scale society and environment. In order to map these impacts, effective monitoring and quantification through the use of high-resolution and up-to-date geospatial information is essential [1]. As such, several land cover (LC) mapping initiatives based on space-borne products have been undertaken. However, a critical analysis on the state of the art conveys that many of the actual methodologies still suffer either from i) the lack of dynamic land mapping capabilities to account for land use changes or ii) limited temporal transferability of the approach. This aspect affects in particular supervised techniques that are based on single images or on sparse sets of dates. The need to overcome such issue has been rapidly pushing the remote sensing community towards solutions based on sensors integration and on dense time series. The use of multiple sensors, especially in the popular synergy between SAR and optical data, is valued both for its enlarged spectral baseline and its temporal revisit enhancements. The paper discusses a statistical approach based on the Hidden Markov Model (HMM) framework first introduced by the authors in [2]. The system, tested so far only on a single sensor datasets (Landsat), performs a dynamic land cover classification for long (several years) and dense time series, efficiently tackling the two aforementioned issues. Nevertheless, some accuracy issues were encountered, especially concerning the confusion between grassland and annual crops, due to the gaps in the Landsat time-series. This paper will hence shed light on the possible strategies to incorporate C-Band SAR data (Sentinel-1 and Radarsat-2 are examined) into the HMM framework and will discuss its benefits in terms of classification results and timeliness for the crop monitoring functionalities, these latter concerning start of growth and harvest detection.

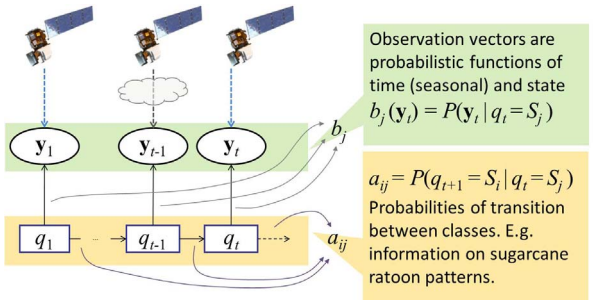

Fig. 1. Schematic representation of the two probabilistic mechanisms involved in a Hidden Markov Model. The underlying hidden sequence of states can be estimated only through their observed output, when this latter is available.

2. THE HIDDEN MARKOV MODELS FRAMEWORK

Hidden Markov models (HMMs) provide a powerful mathematical foundation for modeling the causality relationships in discrete data series. They postulate the presence of two interlinked stochastic mechanisms, as illustrated in Fig. 1: the first regulating the underlying sequence of finite system states, the second describing the observation output probabilities associated to each state. The sequence of states is not known to the user, hence the 'hidden' attribute. Their occurrence can only be tracked through their data output, which will be referred to as 'observations'. In the context of a generic classification problem, the hidden state at each time, or epoch, t represents the class to be estimated, given the whole sequence of available observations. More formally, let denote the N possible states of the system by $S = \{ S_1, \quad S_2, \quad \cdots \quad , S_N \}$, the state at time (or epoch) t as q_t and the M-dimensional obser-

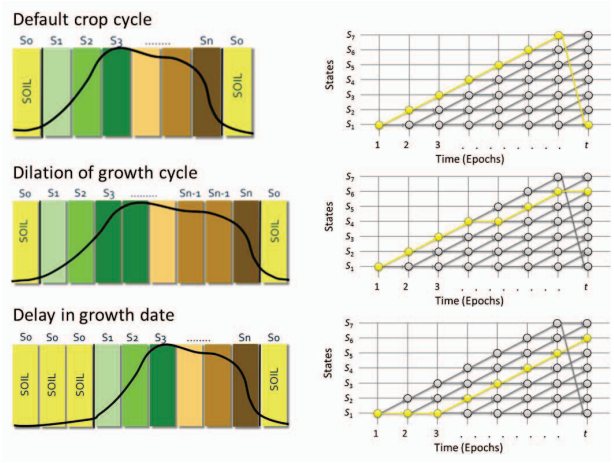

Fig. 2. Example of the technique flexibility to the crop cycle diversity. The Viterbi solution associated to each example is also highlighted in the state-time trellis.

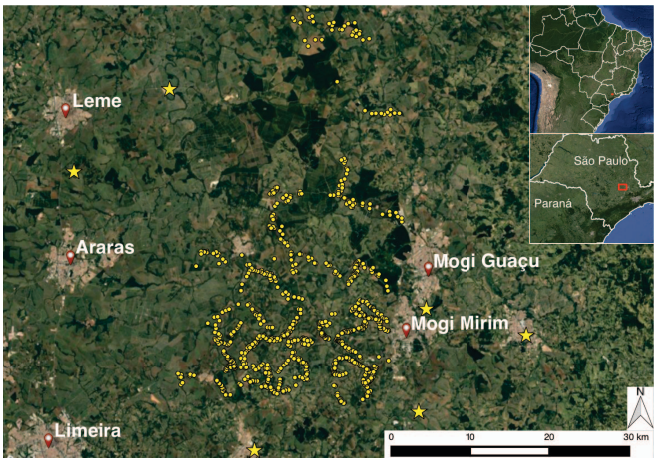

Fig. 3. Study area, indicating the more than eight hundred fields visited with yellow points and the weather stations with yellow stars.

vation vector at time t as $\mathbf{y}_t = \left[\ y_1(t), \quad \cdots \quad , y_M(t)\ \right]^T$. The time series from the two processes are recalled as

$$\begin{aligned} \mathbf{Y} &= \mathbf{y}_1\, \mathbf{y}_2\, \ldots\, \mathbf{y}_T \\ \mathbf{q} &= q_1\, q_2\, \ldots\, q_T \end{aligned} \tag{1}$$

over a time span that accounts for T steps. The order-one chain assumes that each state is only dependent on the previous state. Formally the property reads as $P\left(q_{t+1}\,|\mathbf{q}\right) = P\left(q_{t+1}\,|q_t\right)$. In addition, the model is constrained by the property that each observation is only dependent on its generating state, i.e $P\left(\mathbf{y}_t\,|\mathbf{q}\right) = P\left(\mathbf{y}_t\,|q_t\right)$. As a result the constitutive relationships of a Markov chain process are exhaustively described through the transition probabilities between different states, the emission probabilities for each state and the a-priori information on the state probabilities, denoted respectively $A = \{a_{i,j}\}$, $B = \{b_j\left(\mathbf{y}\right)\}$, and $\pi = \{\pi_i\}$. This element set identifies indeed the hidden Markov model $\lambda = (A, B, \pi)$. The problem of inferring the hidden sequence of states $\hat{\mathbf{q}}$ can be conveniently solved by maximizing the likelihood of the whole sequence through

$$\hat{\mathbf{q}} = \underset{\mathbf{q}}{\operatorname{argmax}} \left\{P\left(\mathbf{Y}, \mathbf{q}\,|\lambda\right)\right\}. \tag{2}$$

Efficient algorithms based on lattice structures are by the well-known 'Viterbi' algorithm, built on dynamic programming concepts. It can be noted that such solution is particularly robust to irregularities in the crop cycle length and in growth time, due to its intrinsic dynamic time warping capabilities as shown in Fig. 2. The reader can refer to [3] to have a mathematical overview on the HMM theory and its practical implementation aspects and to [2] to have a more detailed insight on the model adaptation to the LC monitoring problem.

3. STUDY AREA AND DATA

The test site is located in an area having a variety of land cover types, about fifty kilometers north of the metropole Campinas and close to the medium-sized city Mogi Guaçu in São Paulo state, Brazil, Figure 3. During the two annual crop cycles in 2015, ten ground reference campaigns were carried out, which resulted in the identification of the major land cover types, including sugarcane, corn, soybean, pasture, mandioca (cassava), citrus, eucalyptus, native forest, urban and water. Using the freely available mobile/web application for data collection tool EpiCollect, the location, time, land cover type, vegetation stage, height, additional notes and photo were collected. Subsequently, the more than 800 fields were polygonized based on Google Earth imagery and Landsat-8 NDVI scenes. After digitalization the time span for which the ground validation data is valid (i.e. start of growth and end of growth) was identified using Sentinel-1 HV and Landsat-8 NDVI time series. In addition, daily precipitation data was acquired from six weather stations surrounding the study area.

The remote sensing acquisition scheme, along with the field campaign dates, is shown in Fig. 4 and summarized in Table 1. The remote sensing data characteristics show a range in available wavelengths, polarizations, resolutions and beam angles. It should be noted that Radarsat-2 and Sentinel-1 were multi-looked and over-sampled, respectively, to 30 by 30 meter resolution, and co-registered to the Landsat spatial grid.

4. SAR INTEGRATION STRATEGY

The HMM framework is conceived to handle gaps in the observations, which are typical of optical acquisitions. It was indeed shown that in areas with sufficient clear sky conditions

Sensor[1]	Waveband / wavelength	Mode[2]	Polarizations / bands	Resolution	Revisit / acquisition time[3]	Images
RS2	C-band (5.5 cm)	S5 (ASC & DSC)	HH+HV	7.7 m x 13.5 m	24 days / 21:45 & 08:32	2
		S6 (ASC)			24 days / 21:49	5
		S7 (ASC)			24 days / 20:55	9
S1	C-band (5.5 cm)	EW (DSC)	HH+HV	87 m x 93 m[4]	12 days / 08:38	33
LS8	Optical	Reflectances	RGB+NIR+SWIR1/2	30 m x 30 m	17 days / 10:10	32

Table 1. Characteristics of available remote sensing data. [1]RS2 = Radarsat-2, S1 = Sentinel-1, LS8 = Landsat-8;[2]ASC: ascending pass, DSC: descending pass;[3]UTC, local time -2/-3 hours and approximate times, may change minutes between different operation submodes;[4]Re-gridded by ESA to medium resolution product, original spatial resolution 20 m x 40 m.

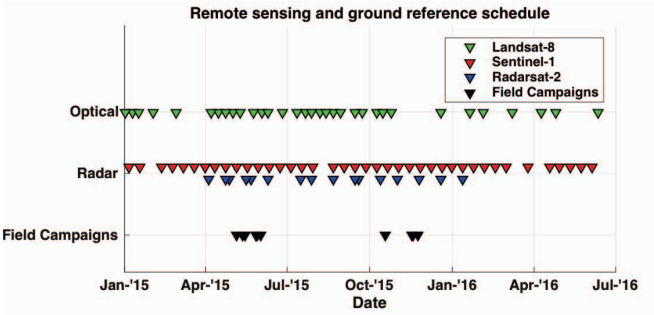

Fig. 4. Remote sensing data availability and ground reference data acquisition scheme.

(say, as a rule of thumb, more than 12 acquisitions per year) Landsat data can achieve, alone, accuracies higher than 85%. However, it is evident that the incorporation of SAR into the methodology would lead to a series of benefits concerning both the discriminative power due to the additional spectral information and the robustness in gap filling. On the other hand, it is also evident that a reliable modeling of the radar response for different types of land covers and land cover conditions is not trivial due to the large fluctuations of the signal response in space and time, as a result of plant geometrical and water content heterogeneities. In order to cope with such complexity, an additional processing module has been hence conceived. The module performs a standalone pre-processing and LC parameter extraction from the SAR time-series. Its core is the tracking of harvest events and vegetation growth conditions.

The statistics of bare soil, harvest events and start of crop growth are extracted for the annual crops and sugarcane, basing on the ground reference data. A set of thresholds and constrained optimization criteria are used to identify, from the SAR data, bare soil and harvest events for each pixel, intuitively associable to thresholded local minima of the signal. The main constraint is the respect of a minimum time distance of three months between the minima. A similar procedure is applied to the maxima based on the signal statistics of the mature stage of annual crops and sugarcane. A simple but effective decision tree approach is then used to carry out the classification. The locations of the minima and maxima are further processed to identify complete growth cycles. The duration of these growth cycles yields the difference between annual crops and sugarcane. As for urban, forests, pasture and citrus, the main requirement is the absence of minima-maxima alternation and the constantly high HV returns, i.e. above the statistically derived threshold. Since the HV-derived statistics were too similar to make a sufficient distinction between the latter classes, the decision tree rules were extended to include yearly averages and maximum seasonal excursions of the NDVI time series. These steps were applied to the available time-series covering around 1.5 years. Such timeframe allowed the detection harvest events for most crops, at least more than two events for annual crops (generally having a crop cycle of 3 to 6 months) and one or two events for sugarcane (generally having a growth cycle of one year with a range of ten to eighteen months). A subset of the map achieved by such SAR-oriented parameter extraction approach is shown in Fig. 5. Two exemplary time series of annual crop (point A) and pasture (point B) are shown on the right where growth cycles for annual crop and seasonality characteristics for pasture. A closer look shows that the increase of HV after harvest (at the local minima) can reach signals at mature crop levels within one or two acquisitions, i.e. within 24 days. More detailed analysis revealed that HV signals from sugarcane saturate during the first 0.5 meter of growth when the signals are taken when the field is wet from rain and up to 1.5 meter when not rain affected. Consequently, although with Radarsat-2 a higher spatial resolution can be obtained, the temporal resolution results in the missing of essential harvest events. The largest errors made with the classification lie in the confusion between pastures and sugarcane due to the similar growth patterns in the same season, i.e. pasture fields that are lightly vegetated due to severe drought or grazing of cows with the same cycle duration of a year as sugarcane are classified as sugarcane, and sugarcane or annual crop is classified as pasture when fields are not properly harvested and remaining stubble or plant material is left. In addition, some confusion exists between the annual crops and sugarcane, when the annual crop fields were not properly harvested and ploughed but remaining vegetation (e.g. grasses) was left after plant removal.

On the base of such ensemble of data and methods, two

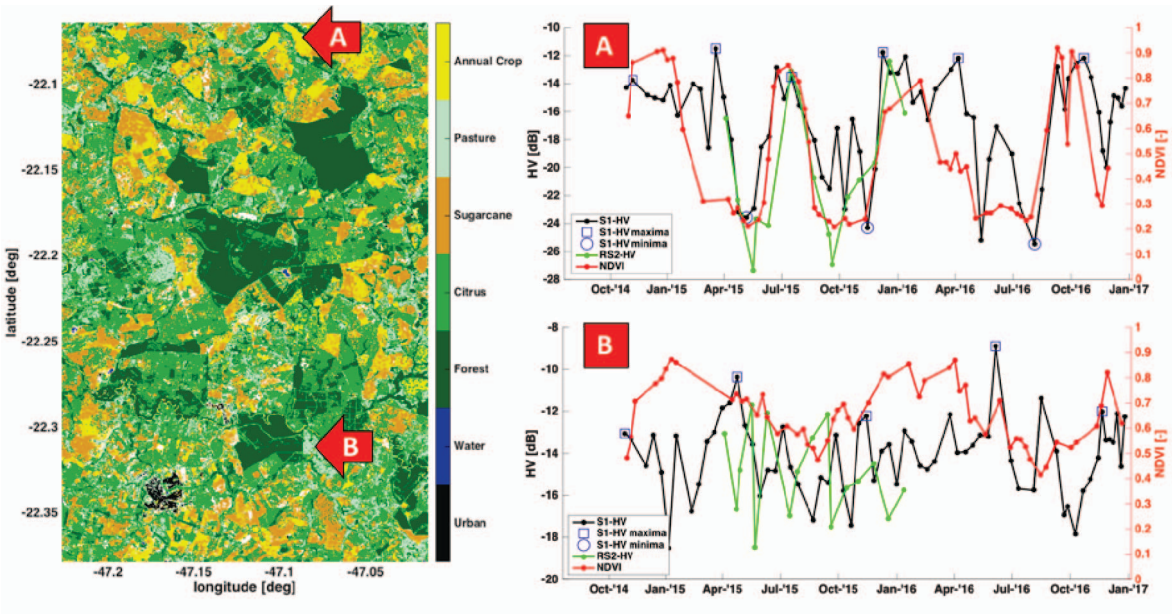

Fig. 5. Classified map of a part of the Mogi Guaçu study area (left) and Sentinel-1 HV and Landsat-8 NDVI time series (right) of the indicated locations.

different approaches for the integration of the SAR and optical datasets can be advocated:

1. A 'State Forcing' approach, where the states q_t of the HMM model are hard-constrained to soil or vegetated status as dictated by the SAR mapping module
2. A 'Mixture-of-Experts' approach, where the land cover results from the Landsat-driven HMM technique and the SAR-based results produced by the independent module are merged on the base of qualitative and quantitative criteria.

Both solutions are based on the information retrieved from the independent SAR mapping module, albeit in a different way. The first approach uses SAR for a pre-filtering, or preselection, of the feasible solutions, $\mathbf{q}$, to be explored by the Viterbi solver. Only the core of the SAR algorithm, i.e. the part related to the tracking of bare soil vs vegetation cover conditions, is retained in such process. Conversely, the second approach assimilates the information in a-posteriori way, more specifically, by trying to mitigate the confusion between pasture and crops, see [2], in the Landsat-driven HMM maps. The strategy consists then in replacing the HMM outcomes with the SAR-based estimates whenever the Likelihood ratio $\frac{P(\mathbf{Y},\mathbf{q}=pasture|\lambda)}{P(\mathbf{Y},\mathbf{q}=crop|\lambda)}$ evaluated on the best HMM pasture/crop sequence candidates is lower than a predetermined threshold.

In conclusion, it shall be registered that the preliminary results show interesting premises for both approaches, since the SAR standalone estimates present significant discrepancies with respect to their optical HMM counterpart. More in-depth and quantitative analysis will hence be conducted.

Acknowledgments

The authors would like to acknowledge the European Space Agency (ESA) for providing the SAR data under the framework of project C1P.16849 and the Brazilian Space Agency (INPE) for kindly supporting our research by providing the Canasat maps of the São Paulo region. The work has been carried out within the framework of the joint BE-Basic FAPESP project: 2013/50943-9.

5. REFERENCES

[1] J. A. Verstegen et al. What can and can't we say about indirect land-use change in Brazil using an integrated economic land-use change model? *GCB Bioenergy*, 8(3):561–578, 2016.

[2] L. Iannini, R. Molijn, A. Mousivand, R. Hanssen, and R. Lamparelli. A HMM-based approach for historic and up-to-date land cover mapping through Landsat time-series in the state of Sao paulo, Brazil. In *2016 IEEE IGARSS*, July 2016.

[3] L. Rabiner. A tutorial on hidden Markov models and selected applications in speech recognition. *Proceedings of the IEEE*, 77(2), 1989.